FEBS Letters 581 (2007) 5597–5600

Glucose-6-phosphate as a probe for the glucosamine-6-phosphate *N*-acetyltransferase Michaelis complex

Ramon Hurtado-Guerrero, Olawale Raimi, Sharon Shepherd, Daan M.F. van Aalten*

Division of Biological Chemistry and Drug Discovery, School of Life Sciences, University of Dundee, Dundee DD1 5EH, Scotland, United Kingdom

Received 5 October 2007; revised 25 October 2007; accepted 26 October 2007

Available online 20 November 2007

Edited by Hans Eklund

Abstract Glucosamine-6-phosphate *N*-acetyltransferase (GNA1) catalyses the *N*-acetylation of D-glucosamine-6-phosphate (GlcN-6P), using acetyl-CoA as an acetyl donor. The product GlcNAc-6P is an intermediate in the biosynthesis UDP-GlcNAc. GNA1 is part of the GCN5-related acetyl transferase family (GNATs), which employ a wide range of acceptor substrates. GNA1 has been genetically validated as an antifungal drug target. Detailed knowledge of the Michaelis complex and trajectory towards the transition state would facilitate rational design of inhibitors of GNA1 and other GNAT enzymes. Using the pseudo-substrate glucose-6-phosphate (Glc-6P) as a probe with GNA1 crystals, we have trapped the first GNAT (pseudo-)Michaelis complex, providing direct evidence for the nucleophilic attack of the substrate amine, and giving insight into the protonation of the thiolate leaving group.

Keywords: Crystal structure; Michaelis complex; Acetyltransferase; UDP-GlcNAc; Kinetics; Inhibitor

1. Introduction

Uridine diphospho-*N*-acetylglucosamine (UDP-GlcNAc) is a key metabolite required for diverse processes such as chitin biosynthesis in fungi [1], the synthesis of glycosylphosphatidylinositol (GPI) anchors of cell wall proteins [2] and the synthesis of *N*-linked and *O*-linked glycans. The UDP-GlcNAc biosynthetic pathway is formed by four enzymes. The first enzyme, glutamine:fructose-6-phosphate amidotransferase (GFA1), is bifunctional, converting fructose-6-phosphate and glutamine to glucosamine-6-phosphate (GlcN-6P) [3]. The second enzyme in the pathway is D-glucosamine-6-phosphate *N*-acetyltransferase (GNA1), which converts acetyl-CoA (AcCoA) and GlcN-6P to CoA and *N*-acetylglucosamine-6-phosphate (GlcNAc-6P) [3]. The third enzyme, GlcNAc phosphomutase, converts GlcNAc-6P to GlcNAc-1P, employing glucose-1,6-bisphosphate as a co-factor [4]. The final enzyme, UDP-*N*-acetylglucosamine pyrophosphorylase, converts UTP and GlcNAc-1P to UDP-GlcNAc and pyrophosphate [3,5].

GNA1 belongs to the superfamily of Gcn5-related *N*-acetyltransferases (GNAT), widely distributed in nature, which use acyl-CoAs to acylate their cognate substrates [6]. Examples of key members of this superfamily include: aminoglycoside, serotonin and glucosamine-6-phosphate *N*-acetyltransferases, histone acetyltransferase, mycothiol synthase, protein α-*N*-myristoyltransferase and the FEM family of acyltransferases [6]. More than 24 crystal structures of members of this superfamily have been solved, and, despite poor sequence conservation, they all have in common a structurally conserved α/β-fold [6]. For the majority of enzymes of the GNAT family, including GNA1, a mechanism involving direct nucleophilic attack of the substrate amine onto AcCoA has been proposed, although uncertainties exist concerning the role of conserved active site cysteines, residues involved in transition state stabilization and the nature of key protonation events along the reaction coordinate [6,7]. For this type of direct attack mechanism, trapping the pre-transition state Michaelis complex is inherently difficult as this cannot be achieved through mutagenesis of the protein, and indeed no such complex has yet been reported for any GNAT member. Here, we report the use of a substrate analogue to approach the structure of the *Aspergillus fumigatus* GNA1 Michaelis complex, which, together with mutagenesis and kinetic analyses, gives insight into the nature of the reaction intermediate and its subsequent protonation.

2. Materials and methods

Expression and purification of *Af*GNA1 were performed as reported elsewhere [8]. Steady-state kinetics of wild-type (WT) and Tyr174Phe mutant were determined using a previous described protocol [9,10] with some modifications. AcCoA and GlcN-6P, and CoA were supplied by Sigma. All measurements were performed in triplicate. Standard reactions consisted of 5 nM *Af*GNA1 (1000 nM for the *Af*GNA1 Tyr174Phe mutant) in 25 mM Tris–HCl, 250 mM NaCl, 2 mM EDTA, 5% (v/v) glycerol, pH 7.5 in a total volume of 50 μl, incubated at RT. The reactions were initiated by adding the protein and stopped with 50 μl of a solution containing 25 mM bis-Tris-propane, 250 mM NaCl, 2 mM EDTA and 6.4 M guanidine chloride, pH 7.5. Fifty microliters of dithio-bis(2-nitrobenzoic acid) (DTNB) solution (1 mM DTNB in 0.1% DMSO) containing 25 mM Tris–HCl, 250 mM NaCl and 2 mM EDTA, pH 7.5 was added and the absorbance at 412 nm determined. Absorbance was quantified using a Spectra max 340 PC (molecular devices). The absorbance data were analyzed with non-linear regression analysis using GRAFIT 5 [11], with the default equations for first order reaction rates and Michaelis–Menten steady-state kinetics. Inhibition of Glc-6P was measured under steady-state conditions using concentrations in the 0–10 mM range while varying the GlcN-6P concentration (500–50 μM) at a fixed AcCoA concentration (500 μM). The Tyr174Phe mutant was generated using the Stratagene QuickChange kit, following the manufacturer's instructions.

*Corresponding author. Fax: +44 (0) 1382 385764.
E-mail address: dava@davapc1.bioch.dundee.ac.uk (D.M.F. van Aalten).

0014-5793/$32.00
doi:10.1016/j.febslet.2007.10.065

The sitting-drop vapor diffusion method was used to produce crystals by mixing 0.6 μl of the protein solution at 17 mg/ml containing 10 mM AcCoA with an equal volume of mother liquor (10–25% PEG 1500; 2.5–15% PEG 1000 and 7.5–22.5% PEG 8000). Bar-shaped crystals (space group $C222_1$) grew within 3 days. *Af*GNA1-AcCoA crystals were soaked in mother liquor containing 30 mM Glc-6P, cryoprotected using mother liquor containing 35% PEG 1000 and 10% PEG 8000, and frozen in a nitrogen gas stream cooled to 100 K. Synchrotron data were collected to 1.45 Å (Table 1). Refinement was started from the native *Af*GNA1 structure [8] using REFMAC [12] interspersed with model building with COOT [13], resulting in a final model with $R = 0.168$ ($R_{free} = 0.219$). Models for ligands were not included until their conformations were well defined by the unbiased $|F_o| - |F_c|$, ϕ_{calc} electron density maps (Fig. 1A). Ligand topologies and coordinates were generated with PRODRG [14]. WHAT IF [15] was used to check hydrogen bonds and PyMol [16] was used to generate pictures.

Table 1
Details of data collection and structure refinement

	*Af*GNA1 + AcCoA + Glc-6P
Space group	$C222_1$
Unit cell (Å)	$a = 70.68$, $b = 100.54$, $c = 55.00$
Resolution range (Å)	20.00–1.45 (1.50–1.45)
# Observed reflections	104265 (9155)
# Unique reflections	33822 (3072)
Redundancy	3.1 (3.0)
$I/\sigma I$	12.2 (2.3)
Completeness (%)	94.2 (86.4)
R_{merge}	0.068 (0.463)
R, R_{free}	0.168, 0.219
RMSD from ideal geometry	
Bonds (Å)	0.012
Angles (°)	1.71
B-factor RMSD (Å^2) (backbone bonds)	
⟨*B*⟩ (Å^2)	1.23
Protein	17.8
AcCoA	16.3
Glc-6	24.2
Water	30.2

Values between brackets are for the highest resolution shell. All measured data were included in structure refinement.

3. Results and discussion

In an attempt to trap the GNA1 Michaelis complex, Glc-6P (carrying a weaker 2-hydroxyl nucleophile instead of the GlcN-6P 2-amino group) was evaluated as an inhibitor against *A. fumigatus* GNA1. Glc-6P displayed weak competitive inhibition ($K_i = 2.6 \pm 0.5$ mM) against the GlcN-6P substrate ($K_m = 71 \pm 6$ μM). Protein crystals of *A. fumigatus* GNA1 (*Af*GNA1) grown in the presence of AcCoA were soaked with Glc-6P, diffraction data to 1.45 Å were collected and the structure of the ternary complex refined (Table 1). Both AcCoA and β-Glc-6P were well defined by unbiased $|F_o| - |F_c|$, ϕ_{calc} electron density maps (Fig. 1A). The thioester carbonyl oxygen is tethered by hydrogen bonds to the main chain nitrogens of Asp130 and Ile131, whereas the Tyr174 hydroxyl is within hydrogen bonding distance of the thioester sulfur. The O2 hydroxyl is coordinated by the Asp165 main chain carbonyl. While there are no interactions with the anomeric hydroxyl (either in α or β configuration), the remaining glucose hydroxyls and phosphate oxygens are tethered by an extensive hydrogen bonding network, also seen in the product complexes published previously (Fig. 1B, [7]), positioning the Glc-6P 2-hydroxyl to within 3.5 Å of the AcCoA carbonyl carbon (Fig. 1A). Strikingly, the angle between the 2-hydroxyl and the AcCoA carbonyl group is 107°, the ideal Bürgi–Dunitz angle for nucleophilic attack on a carbonyl [17]. Thus, the geometry of this pseudo-Michaelis complex provides direct evidence for a GNA1 reaction mechanism involving nucleophilic attack by the substrate amine.

Comparison of the *Af*GNA1 pseudo-Michaelis complex to a previously determined complex of human GNA1 with the products CoA and GlcNAc-6P, gives further insight into the atomic trajectories along the reaction coordinate (Fig. 1B). The carbonyl oxygen and acetyl methyl occupy the same positions before and after catalysis, in agreement with a rotation of the sugar towards the acetyl group (with the C2 carbon shifting by 1.1 Å) and a rotation of the acetyl group towards the sugar (carbonyl carbon shifting by 1.0 Å). The position of the CoA sulfur is essentially unchanged, in both complexes

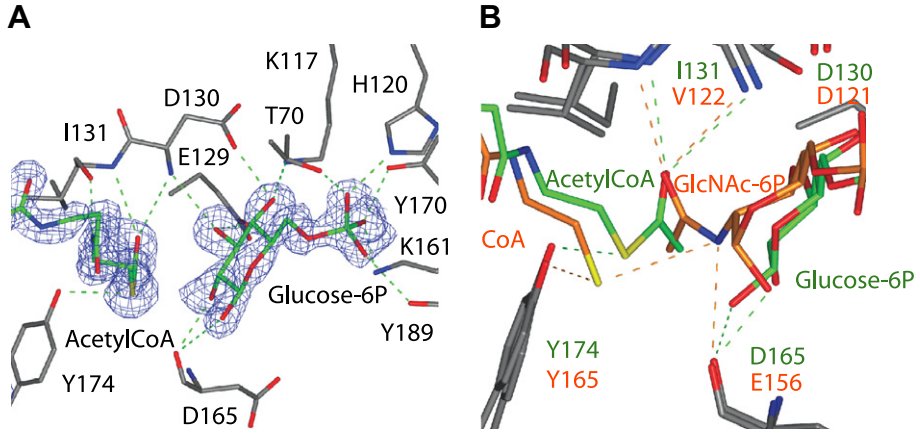

Fig. 1. Structure of the *Af*GNA1-AcCoA/GlcN-6P ternary complex. (A) Detail of the active site of *Af*GNA1 in complex with AcCoA and Glc-6P. Residues lining the active site (grey carbon atoms) and the AcCoA/β-glucose-6P ligands (green carbon atoms) are shown as sticks. Protein-ligand hydrogen bonds are shown as dotted green lines. Unbiased (i.e. before inclusion of any ligand model) $|F_o| - |F_c|$, ϕ_{calc} electron density maps are shown at 2.5σ. (B) Superposition of crystal structures of *Af*GNA1 in complex with AcCoA and Glc-6P onto *Hs*GNA1 in complex with CoA and GlcNAc-6P (PDBID 2O28). The substrates AcCoA and Glc-6P are coloured with green carbon atoms, the products CoA and GlcNAc-6P are shown with orange carbons. Protein-ligand hydrogen bonds are shown as dotted green lines for the substrate complex, and dotted orange lines for the product complex. Residues in the active site are labelled for the substrate complex (green) and the product complex (orange).

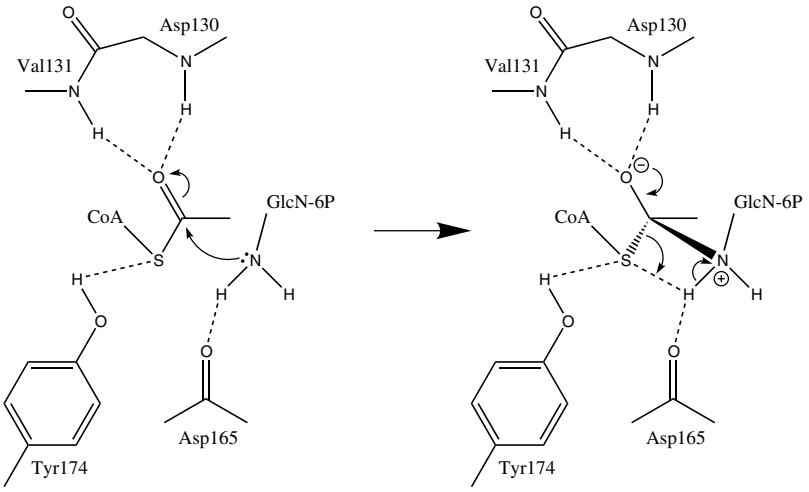

Fig. 2. Reaction mechanism. Details of the reaction mechanism deduced from the pseudo-Michaelis complex, the product complex and mutagenesis data.

within hydrogen bonding distance of the conserved Tyr174, although less ordered in the product complex. For some members of the GNAT family, including yeast GNA1, a similarly positioned tyrosine has been proposed as a proton donor for the thiolate leaving group, based on mutagenesis data [18,6]. Interestingly, the *Af*GNA1 Tyr174Phe mutant shows some remaining activity ($k_{cat} = 0.076 \pm 0.0015\ s^{-1}$ compared to $38 \pm 3\ s^{-1}$ for wild-type *Af*GNA1), and the crystal structure of the mutant AcCoA/Glc-6P complex is indistinguishable from the wild-type complex (data not shown). It is possible that (de)protonation of Tyr174 is not required for catalysis, reducing the role of Tyr174 to stabilisation of the thiolate leaving group, or that in the Tyr174Phe mutant another proton donor takes over the role of Tyr174. Interestingly, inspection of the superposition of the pseudo-Michaelis and product complexes (Fig. 1B) reveals that the backbone oxygen of Asp165 is in a position to interact with one of the hydrogens on the substrate amine, but is also seen to interact with the thiol of the CoA product (Fig. 1B). Strikingly, the Asp165 carbonyl almost perfectly bisects the distance between the acetyl carbonyl carbon positions before and after catalysis and the distance between the thioester sulfur in the substrate and the amide nitrogen in the product. This is an ideal position to facilitate transfer of the surplus proton present on the amine after nucleophilic attack, onto the developing thiolate leaving group (Fig. 2B).

In summary the *Af*GNA1-AcCoA/Glc-6P pseudo-Michaelis complex gives novel insights into structural events along the reaction coordinate (Fig. 2B). The complex shows optimal alignment under the ideal Bürgi–Dunitz angle for direct nucleophilic attack of the sugar amine, and suggests protonation of the tetrahedral intermediate may proceed through intramolecular proton transfer facilitated by a favourably positioned backbone carbonyl. The hydrogen bond established between the hydroxyl group of Tyr174 and the thioester sulfur will increase the electrophilic character of the carbonyl group, favouring the direct nucleophilic attack by the GlcN-6P amine, explaining the 500-fold decrease in the turnover when Tyr174 is mutated to Phe. These insights are applicable to subclasses of other GNAT enzymes and will aid the discovery/design of novel inhibitors.

Acknowledgements: We thank the European Synchrotron Radiation Facility, Grenoble, for the time at beamline BM14. This work was supported by a Wellcome Trust Senior Research Fellowship and the European Union FP6 STREP Fungwall programme. The coordinates and structure factors have been deposited with the PDB (2vez, deposition in progress).

References

[1] Katz, D. and Rosenberger, R.F. (1970) A mutation in aspergillus nidulans producing hyphal walls which lack chitin. Biochim. Biophys. Acta 208, 452–460.
[2] Takeda, J. and Kinoshita, T. (1995) GPI-anchor biosynthesis. Trends Biochem. Sci. 20, 367–371.
[3] Selitrennikoff, C.P. and Sonneborn, D.R. (1976) The last two pathway-specific enzyme activities of hexosamine biosynthesis are present in blastocladiella emersonii zoospores prior to germination. Biochim. Biophys. Acta 451, 408–416.
[4] Hofmann, M., Boles, E. and Zimmermann, F.K. (1994) Characterization of the essential yeast gene encoding *N*-acetylglucosamine-phosphate mutase. Eur. J. Biochem. 221, 741–747.
[5] Etchebehere, L.C., Simon, M.N., Campanhã, R.B., Zapella, P.D., Véron, M. and Maia, J.C. (1993) Developmental regulation of hexosamine biosynthesis by protein phosphatases 2a and 2c in blastocladiella emersonii. J. Bacteriol. 175, 5022–5027.
[6] Vetting, M.W., de Carvalho, L.P.S., Yu, M., Hegde, S.S., Magnet, S., Roderick, S.L. and Blanchard, J.S. (2005) Structure and functions of the gnat superfamily of acetyltransferases. Arch. Biochem. Biophys. 433, 212–226.
[7] Peneff, C., Mengin-Lecreulx, D. and Bourne, Y. (2001) The crystal structures of apo and complexed saccharomyces cerevisiae gna1 shed light on the catalytic mechanism of an amino-sugar *n*-acetyltransferase. J. Biol. Chem. 276, 16328–16334.
[8] Hurtado, R., Plotnikov, A.N. and van Aalten, D.M.F. (in preparation) Structural and kinetic analysis of human and *Aspergillus fumigatus* glucosamine *n*-acetyl transferase reveals exploitable active site differences.
[9] Riddles, P., Blakeley, R. and Zerner, B. (1979) Ellman's reagent: 5,5′-dithiobis(2-nitrobenzoic acid) – a reexamination. Anal. Biochem. 97, 75–81.
[10] Gehring, A.M., Lees, W.J., Mindiola, D.J., Walsh, C.T. and Brown, E.D. (1996) Acetyltransfer precedes uridylyltransfer in the formation of udp-*n*-acetylglucosamine in separable active sites of the bifunctional glmu protein of *Escherichia coli*. Biochemistry 35, 579–585.
[11] Leatherbarrow, R.J. (2001) GraFit Version 5, Erithacus Software Ltd., Horley, UK.

[12] Murshudov, G.N., Vagin, A.A. and Dodson, E.J. (1997) Refinement of macromolecular structures by the maximum-likelihood method. Acta Cryst. D 53, 240–255.
[13] Emsley, P. and Cowtan, K. (2004) Coot: model-building tools for molecular graphics. Acta Cryst. D 60, 2126–2132.
[14] Schuettelkopf, A.W. and van Aalten, D.M.F. (2004) Prodrg: a tool for high-throughput crystallography of protein-ligand complexes. Acta Cryst. D 60, 1355–1363.
[15] Vriend, G. (1990) WHAT IF: a molecular modeling and drug design program. J. Mol. Graph. 8, 52–56.
[16] DeLano, W.L. (2004). Use of pymol as a communications tool for molecular science. Abstr. Pap. Am. Chem. Soc. 228, 030-CHED.
[17] Buergi, H.B., Dunitz, J.D., Lehn, J.M. and Wipff, G. (1974) Stereochemistry of reaction. paths at carbonyl centers. Tetrahedron 30, 1563–1572.
[18] Mio, T., Yamada-Okabe, T., Arisawa, M. and Yamada-Okabe, H. (1999) Saccharomyces cerevisiae gna1, an essential gene encoding a novel acetyltransferase involved in udp-*n*-acetylglucosamine synthesis. J. Biol. Chem. 274, 424–429.